

Relationship between the Morphological Structure and Mechanical Properties of Copper-in-Hydrophilic Polymer Gradient Composite Films

Jianguo Tang, Yanke Che, Haiyan Liu, Yao Wang

Functional Composite Materials Laboratory, College of Chemical Engineering, Qingdao University, Qingdao 266071, People's Republic of China

Received 5 January 2004; accepted 16 July 2004

DOI 10.1002/app.21290

Published online in Wiley InterScience (www.interscience.wiley.com).

ABSTRACT: This investigation was focused on the influence of polymer hydrophilicity on the morphological structure and mechanical properties of copper-in-polymer gradient composite films (CPGCFs). The ion motion and reduction in swelling cathode films under an electric field were the core of the gradient morphology formation of a metal region in the polymer matrix. The morphological study of CPGCFs revealed that the hydrophilicity of poly(vinyl alcohol) was helpful in forming a continuously deposited layer. The nanoclusters (40 nm) aligned into a branchlike form in the copper-rich region in the poly(vinyl alcohol) matrix. On the basis of the fuzzy interface between the poly(vinyl alcohol) matrix and copper nanoclusters, a complex interaction

between them was inferred. The reduced copper affected the mechanical properties of CPGCFs. The maximum load of CPGCFs could be enhanced by 25% to 167.0 N with optimal electrochemical reduction, but the elongation was depressed. An excess of reduced copper in the polymer matrix reduced both the strength and elongation of CPGCFs. The moduli of related samples showed trends similar to those of the strength. © 2004 Wiley Periodicals, Inc. *J Appl Polym Sci* 95: 539–545, 2005

Key words: electrochemistry; morphology; mechanical properties; metal polymer complexes

INTRODUCTION

Materials obtain their ideal properties from their ideal structures. Gradient materials are defined by morphological structures in which the concentrations of two elementary components, such as polymers and metals, change gradually over their cross section. The properties and functions of the materials correspond to their position on the cross section. This gradient morphology is quite effective in reducing interfacial problems.^{1,2} Most successful examples concern metal–ceramic and metal–metal composites.^{3–6} For example, gradient metal–matrix composites offer the advantage of continuously varying mechanical and thermophysical properties, such as the strength, thermal diffusivity, and coefficient of thermal expansion. They are thus considered replacements for protective coatings or multilayered structures in a number of heat-shielding applications, including re-entry space vehicles, space structures, and fusion reactors.⁵ The results indicate that for the same total amount of the ceramic

phase, the heat-shielding capacity is enhanced by an increase in concentration of the ceramic phase at the heated surface, and the temperature gradients inside the plate are affected by the concentration profile of the ceramic region. Wu et al.⁶ pointed out that the laser alloying of a gradient metal–ceramic layer could not only improve the wear resistance of the layer but also prevent the production of cracks. The particles used as hard ceramic regions and incorporated into the layer varied gradually in the volume fraction from the surface to the substrate. The produced layer had a gradient structure and excellent bonding with the substrate and was free of pores and cracks. The microhardness of the gradient layer varied smoothly according to the volume variation of the hard ceramic phase. Obviously, the gradient morphological structures of binary metal or ceramic matrix composites show many advantages.

However, few of these gradient composite studies concern polymer matrices. Actually, the excellent mechanical properties, such as softness and ease of processing, of polymers are really attractive for obtaining ideal functional gradient composites. In our group, a metal-in-polymer gradient composite film (MPGCF) was synthesized by solution reduction synthesis (SRS),^{7–10} by which a swelling cathode film (SCF) was reduced under an electric field. The content of reduced copper changed gradually on the cross section of

Correspondence to: J. Tang (jianguotangde@hotmail.com).

Contract grant sponsor: National Scientific Foundation of the People's Republic of China; contract grant number: 80053001.

MPGCF, and interestingly, the micromorphology of the copper-rich region (CRR) was constructed as a three-dimensional network by reduced copper nanoparticles, which interpenetrated the polymer matrix. Transmission electron microscopy (TEM) results for MPGCF indicated that the copper particle diameter of copper network was about 50 nm.⁷ Ion (i.e., Cu^{2+}) transport and reduction under an electric field are basic electrochemical processes that are different from traditional electrochemical deposition in an aqueous solution. Effective ion motion and reduction to form MPGCF occur in SCF, which is special delivery place with high viscosity, complicated interactions between macromolecular chains and copper ions, solubility of copper(II) ions, and so on. Although we have discussed most of these factors in previous articles,¹¹ the hydrophilicity of polymers as matrices was beyond those investigations. Actually, it is a core fact for determining the dissolvability of copper(II) ions in SCF.

In this study, we investigated the basic aspects of SRS with respect to the hydrophilicity of the polymer matrix, that is, poly(vinyl alcohol) (PVAOH), to prepare MPGCFs.

EXPERIMENTAL

Materials

Commercial PVAOH was purchased from Zibo Synthetic Factory (Zibo, China). Reagent-grade copper chloride was purchased from Tianjin No. 2 Chemical Factory (Tianjin, China). It was dried overnight at 105°C for the elimination of absorbed and hydration water. Deionized water was used as a solvent of PVAOH and copper(II) ions.

Sample preparation

All samples of copper-in-polymer gradient composite films (CPGCFs) were prepared by the electrochemical method; this was similar to our previous articles⁷⁻¹¹ with slight changes. This method consisted of three basic steps. First, the polymer and chloride salt of copper(II) ions (Cu^{2+}) were dissolved in deionized water at $90 \pm 2^\circ\text{C}$ in a vessel for at least 12 h. Second, the solution was coated onto the upper surface of a graphite plate as a cathode. After about 24 h at 20°C, an SCF was obtained. The SCF was reduced electrochemically under the proper electrochemical conditions, which are described in each figure caption.

The structure of the electrochemical reactor was completely the same as that described in ref. 11. In the electrochemical reactor, the anode was a copper disc (diameter = 38 mm), and the cathode was a round and thick graphite plate (diameter = 45 mm), the upper surface of which was coated with the SCF. The thickness of the SCF was about 2 mm. The liquid electrolyte

in the electrochemical reactor was an aqueous solution containing Cu^{2+} and H^+ . An adjustable direct-current power supply unit was used to provide the required direct current.

Measurements

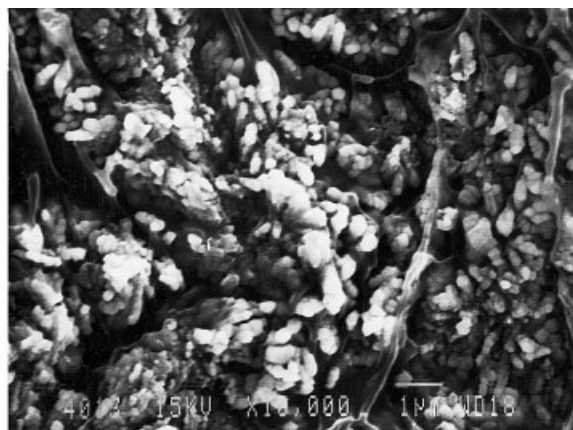
The morphological structure of the CPGCFs was measured with both scanning electron microscopy (SEM) and TEM. The scanning electron microscope was a JEOL JSM-840 (JEOL Co., Tokyo, Japan). The method of calculating the copper content in the films was completely the same as that employed for the previous article.⁷ The transmission electron microscope was a JEM-2000 EX (JEOL Co., Tokyo, Japan). The samples were cut into thin chips (ca. 100 nm thick) with an MT6000 slicer (Sorvall Instruments, United States). In addition to photographs, electron diffraction patterns were also made for the TEM measurements. The Fourier transform infrared (FTIR) information for the CPGCFs was obtained with a Magna-IR 550 FTIR spectrometer (Nicolet Co., Madison, WI). The CPGCF samples were ground into powder and dried at 105°C for 3 h before being mixed with KBr into pellets. The mechanical properties were determined on an Instron multiple mechanical tester (FZY-0102 Automated Materials Testing System, Instron Corp., Canton, MA) at a 10.000 pts/s sample rate, 50% humidity, a 10.000 mm/min crosshead speed, and 23°C. The parameters used for the measurements were a 1.0000-mm specimen thickness, a 15.000-mm specimen gauge length, and a 25.000-mm grip distance.

RESULTS AND DISCUSSION

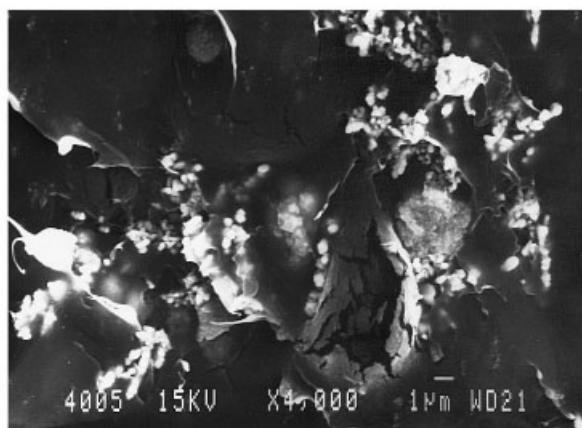
Morphology of the CPGCFs

SEM was used to observe the morphology of the CPGCFs. On the basis of the differences in the topography and atomic numbers between PVAOH and copper, the bright sites on the surface of the cross section were predicted to be CRRs, which were composed of micrometer particles. Figure 1 includes three images corresponding to the deposited, transition, and undeposited portions in the cross section. For the deposited portion, we found condensed and bright CRRs, in which the diameter of the particles was less than 1 μm . Among the CRR areas, there were strips of the polymeric matrix. Figure 1(2) is the image of the transition portion in the cross section: the CRRs were very sparse, but the branches were quite clear. This was a sign of fast electrochemical deposition according to the basic principle of electrochemical deposition theory.¹² It confirmed that PVAOH provided the environment for copper ions to be dissolved and to be transported. On the contrary, the poly(vinyl chloride)

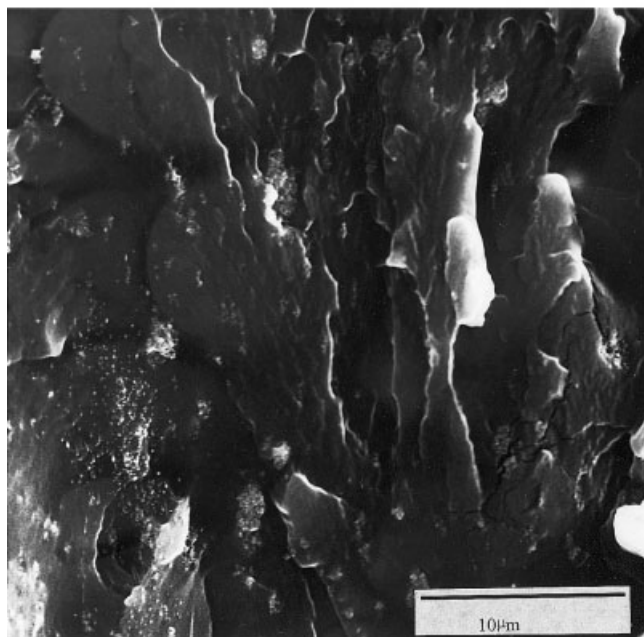
(PVC) in our previous study⁹ supplied weaker dissolvability of the copper(II) ion and produced nanodomain-reduced particles. Figure 1(3) shows the



(1)



(2)



(3)

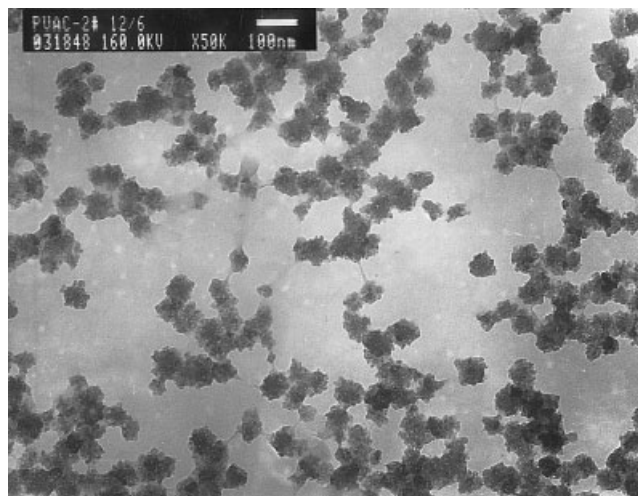


Figure 2 TEM micrograph of CPGCF. The related SCF was reduced under 1 V at 30°C for 4 h, and the original weight ratio of PVAOH to CuCl_2 was 25:20. From the bottom to the top, the nanoclusters aligned into a branchlike image.

undeposited portion in the cross section of the CPGCFs. In this area, reduced copper could hardly be observed.

CRR describes the existence of deposited copper in CPGCFs. It means that the bright sites found by SEM on the surface of the cross section were made up of a subcomposite structure. In Figure 2, nanoclusters of about 40 nm created a branchlike image from the bottom to top. This described the structure in CRR. Paying attention to the interface between the nanoclusters and polymer matrix, we can see that it was fuzzy. That means that there was good interaction between PVAOH and copper. The most likely interaction was a complex between the hydroxyl groups in the main chains of PVAOH and the d -orbital in the copper atoms.¹³

According to our previous investigations,^{7,10} polymers affect the morphological assembly of nanoclusters. Poly(acrylonitrile-*co*-methyl acrylate-*co*-sodium allyl sulfonate) [P(AN-MA-SAS); acrylonitrile/methyl acrylate/sodium allyl sulfonate = 92:6:2 mol/mol/mol] as a matrix generated 50-nm nanoparticles⁷ (Table I), which aggregated into a three-dimensional continuous network interpenetrating with the polymer matrix. However, PVC generated dispersed 10-nm clusters⁹ (Table I) and no deposited layer in the cross

Figure 1 SEM micrographs of (1) the deposited layer, (2) the transition layer, and (3) the undeposited layer. The SCF was reduced under 1 V at 30°C for 4 h, and the original weight ratio of PVAOH to CuCl_2 was 25:20. The first micrograph shows that the deposited layer was constructed of dense and reduced CRRs, the diameters of which 200–800 nm, and thin strips of the PVAOH matrix.

TABLE I
Copper Particle Sizes in Different Polymer (Copolymer) Matrices

Polymer	Size of deposited metal (nm)	Chemical structure analysis	Resources
PVAOH	40	Hydrophilic polymer	Figure 2 in this article
P(AN-MA-SAS)	50	Ternary copolymer	Ref. 8
PVC	10	Hydrophobic polymer	Ref. 9

section of the CPGCFs. Both P(AN-MA-SAS) and PVAOH could generate unique deposited layers in the cross section of the CPGCFs.

Influence of the copper(II) ions on the crystallization of PVAOH

In the FTIR spectra of virgin PVAOH and SCF (Fig. 3), the peak at 1585 cm^{-1} in curve 1 did not occur in curve 2. Because this vibration belonged to O—H bending,^{14–16} it meant that possible interactions between the copper ions and hydroxyl groups, such as complexation and interference with the crystallization of PVAOH, happened. According to the characteristics of complexes between metal ions and hydroxyl groups, the peak often shifted to a lower wave number but did not vanish.¹⁷ However, an increase in the amorphous region made the infrared absorbance diminish or even disappear.¹⁵ Thus, we suggest that the disappearance of the peak at 1585 cm^{-1} was the crystallization depression of PVAOH into which copper(II) ions incorporated. It aided Cu^{2+} ion motion to the

cathode side from the electrolyte, in agreement with the principle that fast ion transport is a characteristic of the amorphous region.^{18,19} This result also agreed with ref. 17, in which several lanthanide chloride salts depressed both the crystallization degree and the crystallization temperature of poly(ethylene oxide).¹⁷

Mechanical properties

The mechanical properties are also important for functional materials. In this research, the morphological structure affected the mechanical properties of the CPGCFs.

The polymer is all important for the mechanical properties of CPGCFs. Flexible units in the polymer or copolymer are very efficient for softening samples. For example, PVC⁹ as a matrix can lead to softer samples than the P(AN-MA-SAS) ternary copolymer. Increasing the soft component in the copolymer, such as methyl acrylate in the P(AN-MA-SAS) ternary copolymer, can effectively improve the flexibility of the composites.¹¹

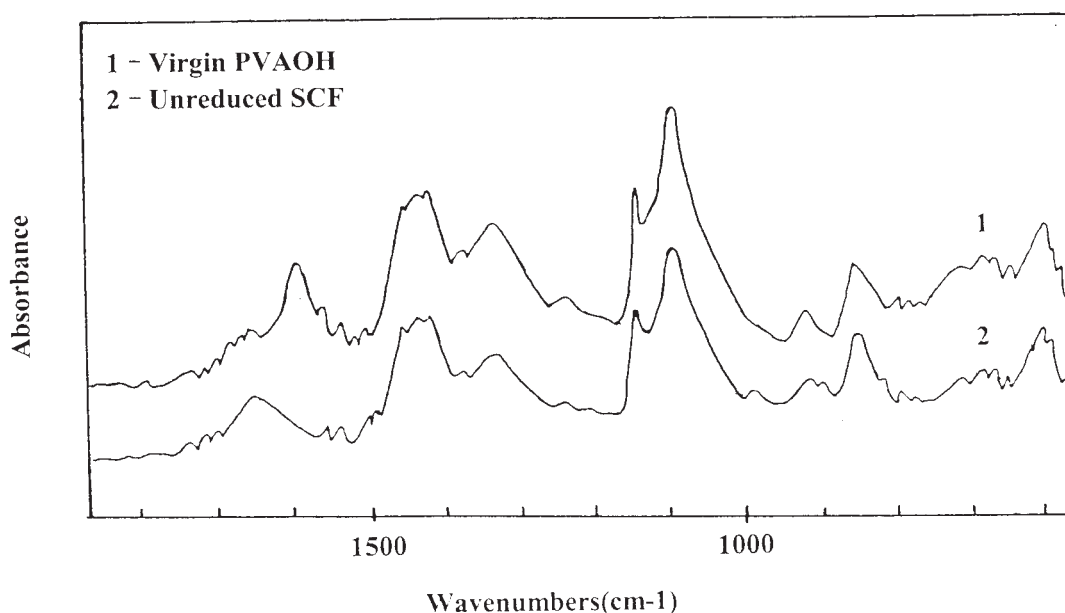


Figure 3 FTIR spectra of (1) PVAOH from an aqueous solution (without copper ions) and (2) an unreduced SCF (with copper ions). The weight ratio of PVAOH to CuCl_2 was 25:10 for curve 2. Both samples were predried for 16 h at the ambient temperature. The second curve indicated no peak at 1585 cm^{-1} .

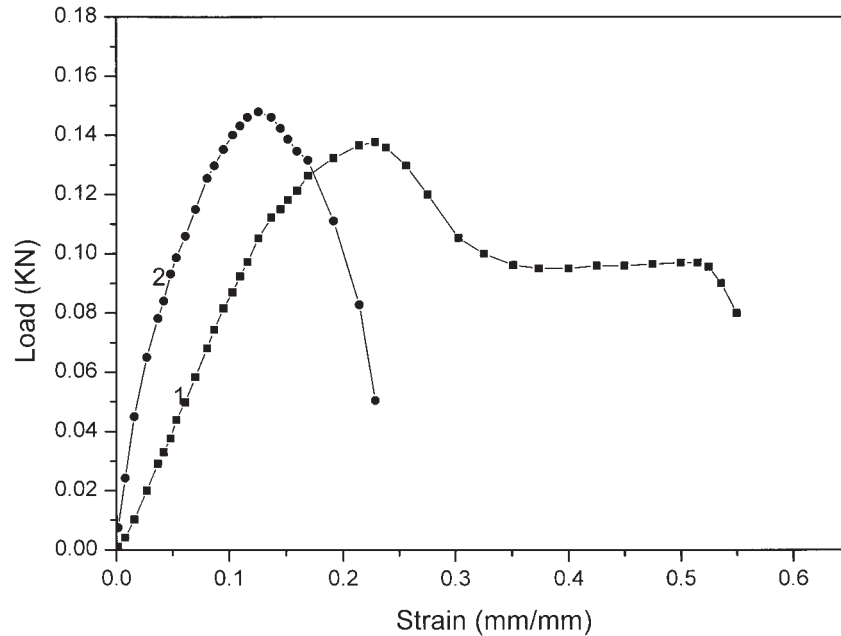


Figure 4 Stress-strain curves of SCFs. The compositions of the original ternary solutions of water, PVAOH, and $\text{CuCl}_2 \cdot 2\text{H}_2\text{O}$ were (1) 7 2.1:18.3:9.6 (w/w) and (2) 68.8:17.4:13.8 (w/w). All the samples were prepared through the casting of ternary solutions onto graphite cathode plates, 20 h of drying at the ambient temperature, and desiccation for several days after they were peeled from graphite plates.

Meanwhile, either the copper ion or reduced copper affected the mechanical properties, whether they dispersed uniquely or gradiently in the polymer matrices. Figure 4 shows that the tested samples for curves 1 and 2 had different concentrations of the copper(II) ion. Figure 4(1) indicates that at a low ion concentration, the sample showed normal stress-strain behavior, which included elastomeric, yielding, and elastic elongations. With an increase in the ion concentration in the samples, the maximum yielding load increased (up to 150.4 N), whereas the maximum yielding elongation decreased [down to 12.47%; Fig. 4(2) and Table II]. The strength enhancement and flexibility depression were due to the complex between the copper ion(II) and hydroxyl groups in PVAOH. This complex provided crosslinks among the macromolecular chains.

On the other hand, the modulus (E) could be calculated according to eq. (1) and the dimensions of the

samples. The calculated E values were $E_1 = 1.16 \times 10^4 \text{ kg/cm}^2$ and $E_2 = 2.68 \times 10^4 \text{ kg/cm}^2$, which corresponded to Figure 4(1,2):

$$E = \sigma / \varepsilon = (F/A) / (\Delta l / l_0) \quad (1)$$

where σ is the stress, ε is the strain, F is the entire force, A is the area of the cross section, Δl is the change in the length, and l_0 is the original length.

The influence of reduced copper in the CPGCFs on the mechanical properties is shown in Figure 5. The stress-strain curves for these samples indicated yielding behavior but no elastic elongation. The concentrations of the copper salt in the original SCFs also influenced those mechanical behaviors. When the ratios of PVAOH to copper(II) salt in the original SCFs were 38:15 (w/w) and 38:20 (w/w), corresponding to curves 1 and 2 in Figure 5, they had similar elongations at the maximum load but different strengths. Curve 1 showed a higher strength of 167.0 N than that (144.4 N) of curve 2. With different reduction potentials, curves 2 and 3 also showed different stress-strain behaviors. Curve 3, obtained under a higher reduction potential (1.25 V), had a lower maximum load value (118 N) and no yielding behavior. The E values corresponding to curves 1–3 were $E_3 = 2.81 \times 10^4 \text{ kg/cm}^2$, $E_4 = 2.24 \times 10^4 \text{ kg/cm}^2$, and $E_5 = 1.57 \times 10^4 \text{ kg/cm}^2$, respectively. The trend was the same as that of their strengths.

Evaluating the data in Figure 5, we considered the relationship between the morphological structure and

TABLE II
Results of Mechanical Tests for Unreduced SCFs (1 and 2) and CPGCFs (3–5)

Specimen	Maximum load (N)	Strain at maximum load (%)
1	133.7	23.07
2	150.4	12.47
3	167.0	13.58
4	144.4	12.53
5	118.0	14.80

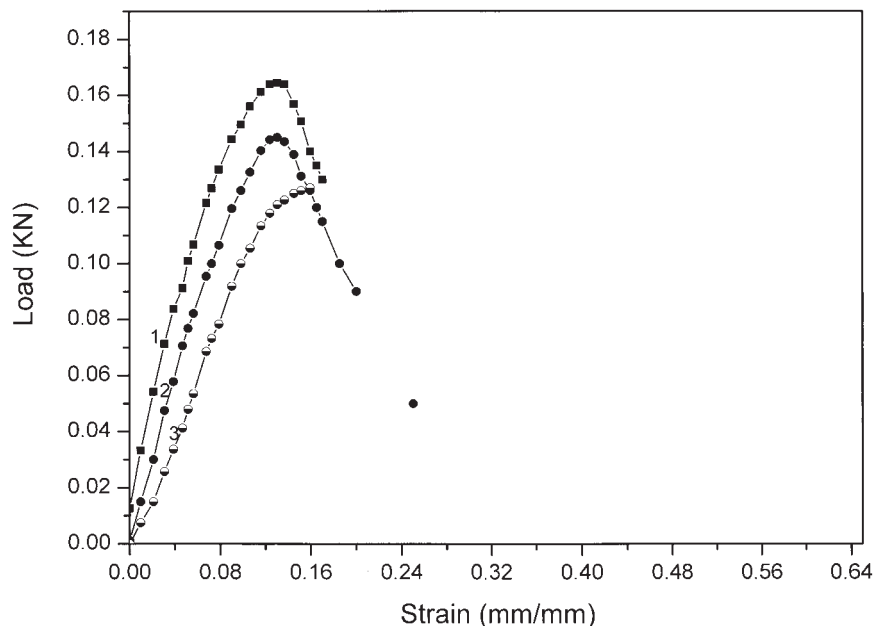


Figure 5 Influence of reduced copper on the stress–strain behavior of CPGCFs. For curves 1 and 2, the samples had for the SCFs the same predrying time of 16 h at the ambient temperature and the same reduction potential of 1 V but different ratios of PVAOH to copper(II) salt (38:15 and 38:20 w/w, respectively). For curves 2 and 3, the samples had the same predrying time for the SCFs and the same ratios of PVAOH to copper(II) salt but different reduction potentials (1 and 1.25 V, respectively).

mechanical properties of CPGCFs. The metal region in the polymer had a branchlike morphology in both the deposited layer and transition layer (Fig. 1).^{7,11} Because of the complex between the hydroxyl groups of PVAOH and the copper nanoclusters [or residual copper(II) ions], the strength of the composite films could be enhanced by more than 25%. The reduced sample in Figure 5(1) and the data of group 3 in Table II showed the highest strength. This confirmed that deposited copper nanoparticles⁷ reinforced the composite film. Figure 6 shows that the broken cross section of the polymer matrix was striplike. Also, we found a broken mark in the metal region from the drawn break. Thus, we suggest that the drawing energy was absorbed by the deformation and breaking of both the polymer strips and metal-rich region. This was the reason that the composite film was reinforced. Unfortunately, the trend did not always follow the increase in the ion concentration and the content of the deposited copper in the polymer matrix (Table II and Fig. 5). The further increases of them in the copper content in the polymer matrix (samples 4 and 5 in Table II and as shown in Fig. 5) diminished both the strength and elongation.

CONCLUSIONS

With hydrophilic PVAOH as the matrix, the cross section of CPGCFs could be divided into deposited, transition, and undeposited portions from the cathode-touching side of the SCF to the other. Thus, it was

confirmed that PVAOH was an excellent medium for dissolving copper(II) ions and providing a microenvironment for ion motion. The CRR in the CPGCFs

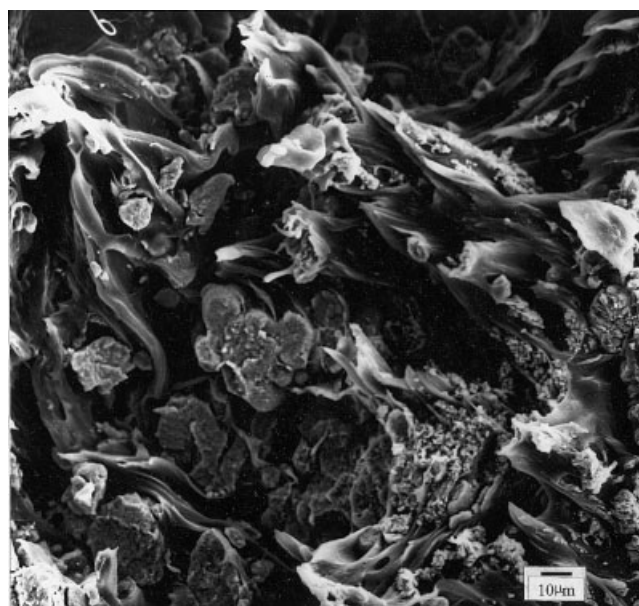


Figure 6 SEM micrograph of a broken cross section of CPGCF drawn via an Instron mechanical test. Both the polymer strands and metal region were broken by the drawing. The drawing energy was absorbed by the deformation and breaking of both the polymer and metal region. The SCF was reduced under 1 V at 30°C for 4 h, and the original weight ratio of PVAOH to CuCl_2 was 25:20.

observed by SEM was constructed of 40-nm clusters embedded in the PVAOH matrix. The interaction between the copper nanoclusters and hydroxyl groups on PVAOH interfered with the crystallization of PVAOH and controlled the morphological formation of CPGCFs. The hydrophilicity of the polymer matrix (PVAOH) determined the dissolvability and thus the ion motion and reduction of the copper(II) ions in the SCF. The reduced copper in CPGCFs affected the mechanical properties. The maximum load could be enhanced by 25% to 167.0 N under optimal electrochemical reduction, but the elongation was depressed. An excess of copper in the polymer matrix decreased both the strength and elongation of the CPGCFs. The E values of related samples showed the same trend as their strengths.

References

1. Mortensen, A.; Suresh, S. *Int Mater Rev* 1997, 42, 85.
2. Freudenstein, R.; Reinke, S.; Kulisch, W.; Fischer, R.; Zweck, J.; Bergmaier, A.; Dollinger, G. *Mater Sci Forum* 1998, 287, 259.
3. Voevodin, A. A.; Zabinski, J. S. *Diamond Relat Mater* 1998, 7, 463.
4. Voevodin, A. A.; Walck, S. D.; Zabinski, J. S. *Wear* 1997, 203, 516.
5. Papathanasiou, T. D.; Soininen, R.; Caridis, K. A. *Scand J Metall* 1995, 24, 159.
6. Wu, P.; Zhou, C. Z.; Tang, X. N. *Surf Coat Technol* 1995, 73, 111.
7. Tang, J. G.; Hu, K. A.; Guo, D. *J Appl Polym Sci* 1999, 74, 1927.
8. Tang, J. G.; Hu, K. A.; Fu, S. H. *J Appl Polym Sci* 1998, 69, 1159.
9. Tang, J. G.; Hu, K. A.; Liu, H. Y. *J Appl Polym Sci* 2000, 76, 1857.
10. Tang, J. G.; Chu, X. F.; Xiao, X.; Zhao, W. Y. *J Appl Polym Sci* 1996, 61, 1773.
11. Tang, J. G.; Chen, Q.; Liu, H. Y.; Wang, Y. *J Appl Polym Sci*, 2004, 92, 373.
12. Paunovic, M. *Fundamentals of Electrochemical Deposition*; Wiley: New York, 1998.
13. Ciardelli, F.; Tsuchia, E.; Wöhrle, D. *Macromolecule-Metal Complexes*; Springer-Verlag: Berlin, 1996.
14. Dai, L. X.; Ying, L. N. *Macromol Mater Eng* 2002, 287, 509.
15. Rao, L.; Jie, X.; Zhang, R. Y. *J Appl Polym Sci* 1994, 53, 325.
16. University of Cincinnati, College of Engineering. <http://www.eng.uc.edu/~gbeaucag/classes/analysis/chapter5.html>. (accessed June 2004).
17. Tang, J. G.; Lee, K. S. C.; Belfiore, L. A. *J Polym Sci Part B: Polym Phys* 2003, 41, 2200.
18. Croce, F.; Appetecchi, G. B.; Persi, L.; Scrosati, B. *Nature* 1998, 394, 456.
19. Joo, C. G.; Bronstein, L. M.; Karlinsey, R. L.; Zwanziger, J. W. *Solid State Nucl Magn Reson* 2002, 22, 235.